Proceedings of ISINN-30, JINR, E3-2024-42, Dubna, 2024, p.11 – 24

Characteristic Features of Double and Triple Coincidence Spectra Coupling in Radiative Neutron Decay

Khafizov R.U.[a], Kolesnikov I.A.[a], Nikolenko M.V.[a], Tarnovitsky S.A.[a], Tolokonnikov S.V.[a], Torokhov V.D.[a], Trifonov G.M.[a], Solovei V.A.[a], Kolkhidashvili M.R.[a], Konorov I.V.[b]

[a]*NRC «Kurchatov Institute», Russia*
[b]*Technical University of Munich, Munich, Germany*

khafizov_ru@nrcki.ru

The paper uses the example of radiative neutron decay, which we discovered in 2005 at the TUM (Technical University of Munich) reactor, to examine the coupling of double and triple coincidence spectra. To this end, special attention is paid to the electronic system for collecting and processing information received from the electron, proton, and gamma-ray detectors. As demonstrated, in the presence of a significant background gamma-ray, the spectrum of triple coincidences will have, apart from the peak of triple coincidences of the beta electron, proton, and gamma-ray quantum, additional peaks which represent responses to the peaks in the spectra of double coincidences of beta electron with proton and beta electron with gamma quantum. After processing the spectra using the response function method, we measured the main characteristic of the radiative beta decay of the neutron, namely its branching ratio. Thus, in this experiment we were the first to measure the branching ratio (B.R.) of radiative neutron decay B.R.= $(3.2\pm1.6)\cdot10^{-3}$ (where C.L.= 99.7% and gamma quanta energy threshold is equal to 35 Kev) [1]. On the other hand, theoretical calculations of this value according to the Standard Model give 1.5 times lower value, so we recorded additional gamma quanta which are structural gamma quanta emitted by the quarks that a neutron consists of.

Introduction

The study of neutron radiative decay is essential for the further development of the atomic project as it creates a new basis for advancing the controlled nuclear fusion. In our recent experiment to measure the relative intensity B.R. of neutron radiative decay we discovered extra gamma quanta produced during neutron decay with the bremsstrahlung gamma quanta emitted from the regular beta decay products. These extra gamma quanta are structural gamma quanta; they carry information about the quark structure of the neutron and are formed during the u and d quarks transition.

Below (see Fig. 1) follow the Feynman diagrams describing neutron decay. The first diagram describes the usual beta decay of the neutron, which produces three particles: a beta electron, a proton, and an antineutrino. This diagram describes the main mode of neutron decay. In the experiment we recorded the number of such decays by the number of double coincidences of the electron and the proton N_D. However, in any decay with the formation of charged particles there is a so-called radiative decay mode, in which, in addition to the regular decay products, an additional particle, a gamma-quantum, is recorded. This additional radiative gamma quantum is a bremsstrahlung gamma quantum emitted from a charged

particle which is flying in the bremsstrahlung electric field of another charged particle. In case of neutron beta decay, bremsstrahlung gamma quanta can be emitted from proton (second diagram in Fig. 1) and beta electron (third diagram in Fig. 1). However, there is still a possibility of gamma emission, which occurs when the structure itself of the elementary particle changes. In the case of neutron decay this process is shown in the fourth diagram in Fig. 1, when gamma-quantum is emitted from the very top of the decay at the transition of u and d quarks included in the structure of neutron and proton. In the experiment, we recorded the number of radiative decay events of the neutron by triple coincidences of electron, proton, and gamma-quantum N_T.

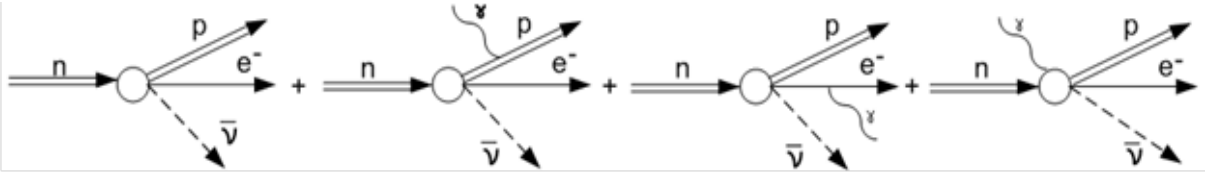

Fig.1. The diagrams describing ordinary beta decay and neutron decay with gamma-quantum emission.

The main characteristic of elementary particle decay is its relative intensity, branching ratio (BR):

$$BR = I(\text{radiative decay}) / I(\text{ordinary decay}) = N(e,p,\gamma) / N(e,p)/k = N_T / N_D/k,$$

where the numbers of triple N_T and double N_D coincidences should be taken directly from the experimental spectra of triple and double coincidences, so that a determination BR indeed reduces to measuring the spectrum of e-p double coincidences and the spectrum of e-p-γ triple coincidences. Without performing an analysis of these spectra, it is impossible to evaluate the branching ratio BR. An additional coefficient k is the so-called geometric factor. It takes into account the geometry of the experimental facility used. The geometric factor k is determined by means of a Monte Carlo simulation of the experiment using the package of CERN programs GEANT IV.

Until recently, the rare radiative mode of neutron decay was not discovered and was considered only theoretically [1–4]. Our first attempt at detecting events of radiative neutron decay was undertaken at the Institut Laue–Langevine (ILL) in employing an intense cold-neutron beam [5]. The experiment that our group performed in 2005 at the FRMII reactor of the Technische Universität München became the first experiment that resulted in observing this process [6]. We were the first to identify events of radiative neutron decay by means of triple coincidences in which an emitted gamma-quantum was recorded as a third particle in addition to the electron and recoil proton. Thus, we were able to measure the branching ratio for the radiative mode of neutron decay. The result was B.R.= $(3.2\pm1.6)\cdot10^{-3}$ at a coincidence level of C.L.=99.7%, the gamma energy being in excess of 35 keV. In the experiments performed earlier at ILL [6] our group was able to measure only the upper limit on this branching ratio. A year later, a group of experimentalists from the National Institute of Standards and Technology (NIST) published in Nature the results of their experiment devoted to studying radiative neutron decay [7]. Their result was B.R.= $(3.13\pm0.34)\cdot10^{-3}$ at C.L.= 68%, the gamma energy there ranging between 15 and 340 keV. However, there were no triple coincidences in this experiment but only the spectra of double coincidences of electron–gamma-quantum and electron–ion. Obviously, without registering exactly the triple coincidence of electron, gamma-quantum, and proton, it is impossible to talk about registering

the events of neutron radiative decay. Such double coincidences occur during the well-studied process of ordinary ionization of the residual gas by electrons in the chamber, as a result of which a glow appears. For example, in nature such a phenomenon is observed as the polar lights at the edge of the atmosphere. The authors of this [7] and later work [8] recorded this radiation of gamma quanta in the hard and invisible area of the spectrum, they had created the ideal conditions for this. There, as will be shown below, was a strong magnetic field, and highly rarefied residual air in the chamber, and ionizing particles (beta-electrons). In addition, the authors of this work recorded ions instead of protons, because due to the strong magnetic field they were not able to distinguish protons and the large ionic background occurring in the experimental facility. Thus, the BR value given by the authors of [7] is the ratio of the intensity of gamma emission during the ionization of rarefied air molecules to the total number of ionization acts by beta-electrons.

Experimental facility

The layout of the proposed experimental facility is shown in Fig. 2. Passing along a rather long neutron guide equipped with a collimating system formed by LiF diaphragms, an intense beam of cold neutrons enters a vacuum chamber (1) through the last LiF diaphragms (9) positioned immediately in front of the decay zone being studied. The decay zone is viewed by detectors of three types simultaneously. These are a proton detector (3) formed by microchannel plates (MCP), an electron detector (13) formed by photomultiplier tubes 7 cm in diameter covered with a scintillator plastic 3 mm thick, and six gamma detectors (11). These six detectors surround the electron detector (see the lower panel in Fig. 2) at an angle of 35° and are formed by photomultiplier tubes covered with a sensitive CsI layer. The layer thickness is 4 mm. It is chosen in such a way that the gamma-quantum detection efficiency is equal to unity. Six gamma detectors (11) surround the electron detector (13) (see the lower panel in Fig. 2) are arranged at an angle of 35° and are protected by a cup (12) made of 6-mm lead. In principle, coincidences between the electron detector and any of the six gamma detectors can completely suppress the background of bremsstrahlung, which arises only in that section where electrons are detected. From Fig. 2, it can be seen that, in this case, part of the data is lost. However, the neutron-beam intensity of 10^{12} n/c/cm^2 in our chamber is quite sufficient in order to compensate for this loss and to retain an acceptable data-accumulation rate. Recoil protons produced in the decay zone travel through the space surrounded by a cylindrical time-of-flight electrode (7) toward the proton detector (3). After that, they are focused on this detector by means of spherical focusing electrodes (2). The focusing electrostatic field is generated between high-voltage spherical (2) and cylindrical (7) electrodes and grids (6 and 5), on one hand, and the underground proton-detector grid (4), on the other hand. It is noteworthy that recoil protons fly isotropically out of the decay vertex. An additional grid (10) is positioned on the opposite side of the decay zone in order to avoid the loss of protons that go toward the electron detector.

A signal from an electron detected in the scintillator plastic of the electron detector (13) serves a start signal that opens all time windows for all detectors. A pulse from one of the gamma detectors (11) is recorded simultaneously with this signal, but only in the case where a signal from the proton detector (3) is generated within a reasonably short time interval will this electron– gamma-quantum coincidence be recorded by an electronic system for data acquisition and data processing as an event of radiative neutron decay. Along with these triple coincidences, our electronic system records ordinary electron–proton coincidences. It should be noted that, in the case of radiative decay, the emitted gamma-quantum is detected in our

facility by the gamma detectors (11), which are placed around the electron detector (13), earlier than the electron is detected by the electron detector (13). In other words, the electron should be delayed with respect to the emitted gamma-quantum in the time spectrum of triple coincidences but by an extremely small amount, e.g., a nanosecond. It is precisely this fact that will enable us to identify the peak associated with radiative gamma quanta in the spectrum of triple coincidences. In addition to triple coincidences, our setup also collects double coincidences corresponding to ordinary neutron decay. Here, it is worth noting that a very high quality of the system of diaphragms from LiF ceramics is necessary to obtain an acceptable low level of the background in gamma quanta from an intense cold-neutron beam while passing this beam through the whole facility from the entrance window to the thick LiF ceramic target absorbing it. The entrance window and the absorbing target are the main sources of gamma background in the facility, therefore the neutron guide must be long enough and its axis must coincide with the beam axis as precisely as possible. In our case, the entrance window for the beam was at a distance of 7 meters from the area viewed by the detectors, and the absorbing target was 3 meters. In the next section we will use the time

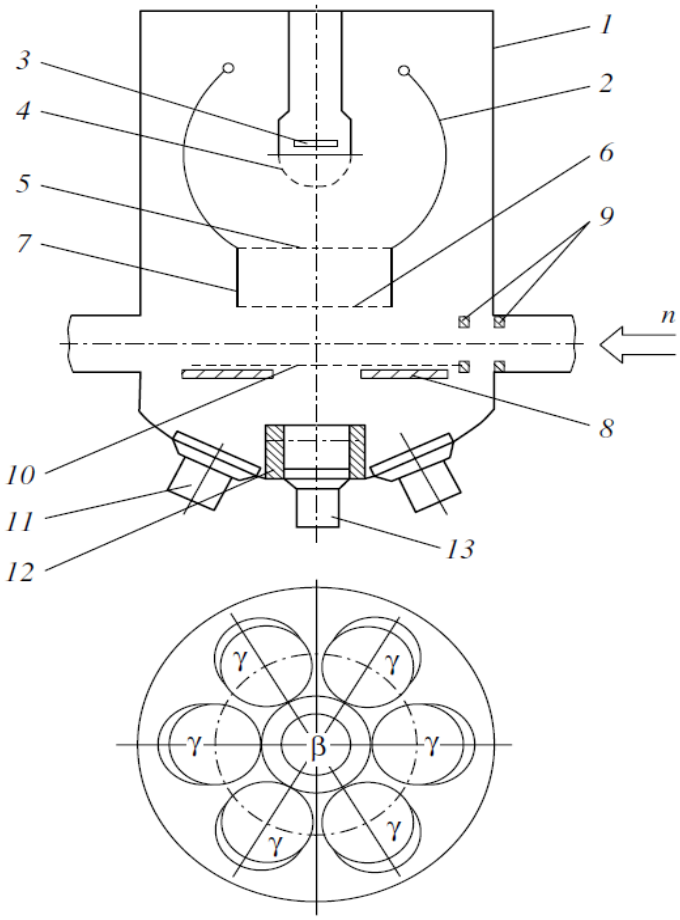

spectra of double and triple coincidences to obtain the experimental value of the main characteristic of the radiative neutron decay (BR).

Fig. 2. Layout of the experimental facility: (1) vacuum chamber, (2) high-voltage (18 to 20 kV) spherical electrodes for focusing recoil protons, (3) proton detector, (4) grid of the proton detector (underground), (5, 6) grids of the time-of-flight electrodes, (7) time-of-flight electrode (at a voltage of 18 to 20 kV), (8) plastic collimator (5 mm thick and 70 mm in diameter) for beta electrons, (9) LiF diaphragms, (10) grid for rotating recoil protons in the backward direction (at a voltage of 22 to

26 kV), (11) six photomultiplier tubes for CsI(Tl) gamma detectors, (12) lead cup, and (13) photomultiplier tube equipped with a plastic scintillator for detecting electrons.

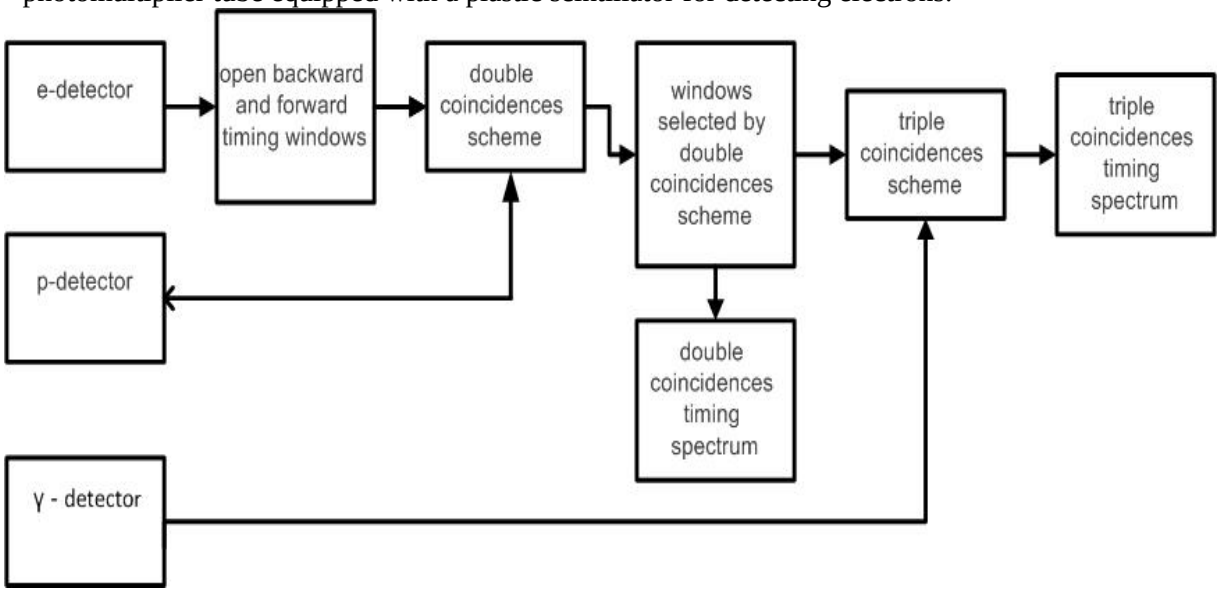

Fig. 3. Flowchart of the electronic system of information collection and processing.

Let us now consider the flowchart of our electronic system for collecting and processing information obtained from detectors of three types – electron detector, proton detector and gamma-ray detector. The flowchart is given in Fig. 3. The signal coming from the electron detector opens time windows 150 channels forward and 100 channels backwards; the scale division value of each channel is 25 nanoseconds. Then the electron-proton double coincidences scheme receives a signal from the proton detector into the corresponding channel opened by a signal from the electronic window detector. As a result, firstly, the spectrum of double time coincidences is formed, and secondly, the windows of double coincidences are selected and fed to the triple coincidences scheme. It should be noted here that the proton detector registers not only protons from beta decay proper but also a great number of ions formed in the experimental chamber and captured by the electrostatic field of the focusing electrodes. As a result, the beta-decaying proton peak must be observed on a significant ion background forming a horizontal substrate under this peak. The height of this substrate is comparable to the height of the proton peak itself. In addition, a high and narrow electron registration response peak should form in the starting channel on the triple coincidences spectrum; the nature of this peak is not physical and is related to the electronic scheme of the double coincidences. Thus, the double coincidences spectrum is a horizontal substrate of background ions with two peaks: the electron registration response peak and the beta decay peak consisting of neutron beta decay protons. The triple coincidences scheme is then fed with signals from six gamma detectors, which in turn are registered in their channels in the time windows selected by the double coincidences scheme, open for 150 channels forward and 100 channels backwards. As a result, a spectrum of triple coincidences is formed where the gamma background is even more significant in its magnitude than the ion background. Due to this uncorrelated background, all the peaks that are observed in the double coincidences spectrum will be displayed, and these two peaks, the electron registration response peak and the beta decay peak, will appear in the triple coincidences spectrum. Besides, additional peaks from the electron-gamma coincidence spectrum will be added to

these two peaks. There are also two such peaks and both of them have a physical nature. The first narrow peak is the peak of radiation gamma quanta, it should be located to the left of all other peaks because radiation gamma quanta are registered before all other particles. The second broad peak comes with a delay of 1 μs and it is formed by gamma quanta from ionizing radiation caused by beta-electrons. It is to be noted that there is residual air in the experimental chamber, the density of which is comparable to the air density at the edge of the earth's atmosphere, where the well-known aurora borealis occurs. Thus, the radiation peak will be observed against an inhomogeneous background in which, in addition to the horizontal substrate, there are three peaks: the peak response to electron registration, the response to the beta decay peak, and the response to the broad peak of the "aurora borealis". In this case, the radiation peak should be located the very first, which is what we observed in the experiment. Looking ahead, we will say that on the real spectrum in channel 116, we observed one more peak, the nature of which is purely electronic, it has nothing to do with physics. The point is that gamma signals have very long "tails", which were "cut off" by the electronic system to reduce the load on them. Below we will consider in detail the obtained spectra of double and triple coincidences.

Timing spectra of double and triple coincidences

Here we will analyze the spectra of double coincidences between beta-electron and proton, and also the spectra of triple coincidences between beta-electron, proton and gamma-quantum. We will compare our results with the results obtained by two other groups from NIST.

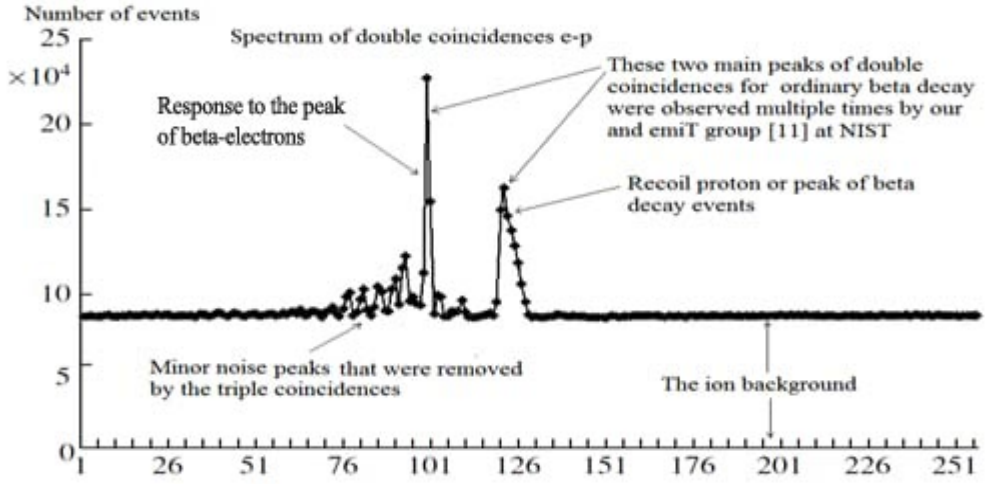

Fig. 4. Timing spectrum for e-p coincidences. Each channel corresponds to 25 ns. The peak at channels 99–100 corresponds to electron registration by the electronic system. The coincidences between the decay electrons and delayed protons (e-p coincidences) are contained in the wide peak centered at channel 120.

Fig. 4 demonstrates the summary statistics on double e-p coincidences (coincidences of a light beta-electron moving at a speed comparable to the speed of light and a delayed heavy proton, whose speed is much lower and is determined by the potential of the accelerating electrostatic field). Therefore, Fig. 4 clearly shows two major peaks: one peak with a maximum in channels 99–100, which is the response to electron registration by the electronic registration and recording system [5, 6] of the experimental facility. The position of

this peak determines the arrival time of the signal from the electron detector, which consists of PMTs and is coated with scintillation plastic. This peak is not physics-related in its nature. Instead, it is a response to the registration of the electron. As soon as the electronic system registers an electron, it opens a time window of one hundred channels forward and backward in time. Thus, the 100th channel is the master channel, and each channel corresponds to 25 nanoseconds, so the spectra can view all events in 2.5 μs before and after the arrival of the electron. The next peak visible on Fig. 4 has a maximum in channel 120, it is physics-related in its nature and is a proton peak, i.e. the peak of e-p coincidences of beta-electron with delayed proton. Its position determines the time of proton registration by the electronic system, and the distance between these two peaks determines the proton delay time.

An analogous situation was first noted in [9], then it was observed during the experiment on the measurement of the correlation coefficients by the group at ILL [5,10] and emiT group at NIST [11], and it was also mentioned at [12]. We would especially like to emphasize the correspondence of our spectrum of double coincidences with an analogous spectrum from the result obtained by the emiT group from NIST [11]. In Fig. 5 we present their spectrum and diagram for the registration of the beta electron and the recoil proton. A comparison of our results with the results of the emiT group shows their unquestionable similarity. Moreover, the position of the second proton peak in Fig. 4 (emiT group), like in Fig. 3 (our result), corresponds well to the simple estimate obtained by dividing the length of a proton trajectory by its average speed.

Here we will also note the presence of a significant homogenous ionic background in Figs. 4 and 5. However, in both cases this background allows to easily distinguish the neutron decay peak, and thus, we can easily determine the number of N_D double coincidence events, i.e. the number of registered neutron beta decays. Note the most important point in the methodology of the experiment: this large ionic background cannot be distinguished from the small number of neutron decay protons (i.e. from beta decay events) in the presence of strong magnetic fields, and thus N_D cannot be determined.

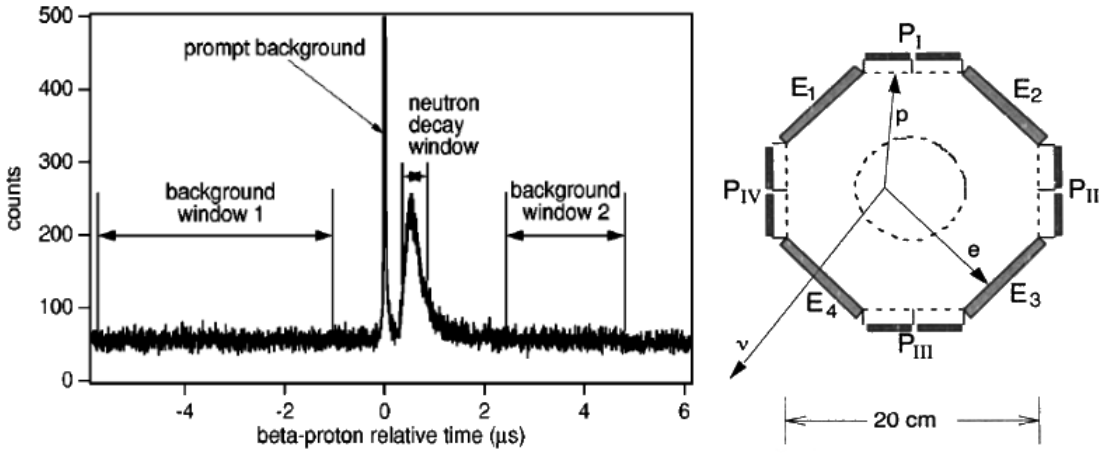

Fig. 5. On the left: spectrum of double electron-proton coincidences obtained by emiT group [11] with two peaks and a significant ion background value comparable to the neutron decay peak; on the right: emiT group scheme for registering beta electron and recoil proton.

Following Avogadro's law, even in the case of a very deep vacuum under pressure of 10^{-6}–10^{-8} mbar, air molecule concentration remains very high. In fact, it is sufficient for beta-electrons produced in neutron decay to create a significantly high ionic background in the chamber, exceeding the number of decay protons by many orders of magnitude. These ions

create a homogeneous background in the absence of strong magnetic fields, throughout the whole spectrum of double coincidences. It should also be noted that the concentration of ions in the chamber does not fall in proportion to the pressure, but much more gradually, as the cubic root of the pressure. Here one must note that the probability of ion creation along the trajectory of beta-electron is in inverse proportion to the average distance between neighboring ions, i.e. is proportional not to the molecule concentration but to the cubic root of this value. This fact means that the ionic background remains significant even when the pressure is reduced by a factor of 100, which is observed when comparing our results with those of the emiT group. The emiT group's vacuum was two orders of magnitude greater, but the ionic background dropped only 4–6 times compared to ours. This estimate is confirmed when one compares the spectra in Figs. 3 and 4. Our spectrum, presented on Fig. 3, has a 1:1 ratio of the value of e-p coincidences peak and the value of the background. The emiT group (Fig. 4) spectrum has a ratio of 4:1 – 5:1, i.e. only 4–5 times our number, that is equal to the cubic root of 100.

Fig. 4 shows that the total number of events in e-p coincidences peak in our experiment equals $N_D=3.75\cdot10^5$. This value significantly exceeds the value we obtained in our previous experiment conducted in ILL. At that time, due to the low statistics volume we could not identify the B.R. itself and instead defined only the upper B.R. limit [5]. So, in both cases Figs. 4 and 5 show not one but two peaks above the homogeneous ionic background.

The remaining peaks on Fig. 4 are small, with just seven peaks distinct from the statistical fluctuations. These occurred because of the noise in the electric circuits of the FRMII neutron guide hall. There are no other physics-related reasons for their occurrence. The fact is that our experiment was the first at the newly opened FRMII reactor, and the neutron guide hall was still undergoing intensive commissioning work. These peaks were appearing during the working days and disappearing over the weekends. Such behavior was observed as we collected statistics.

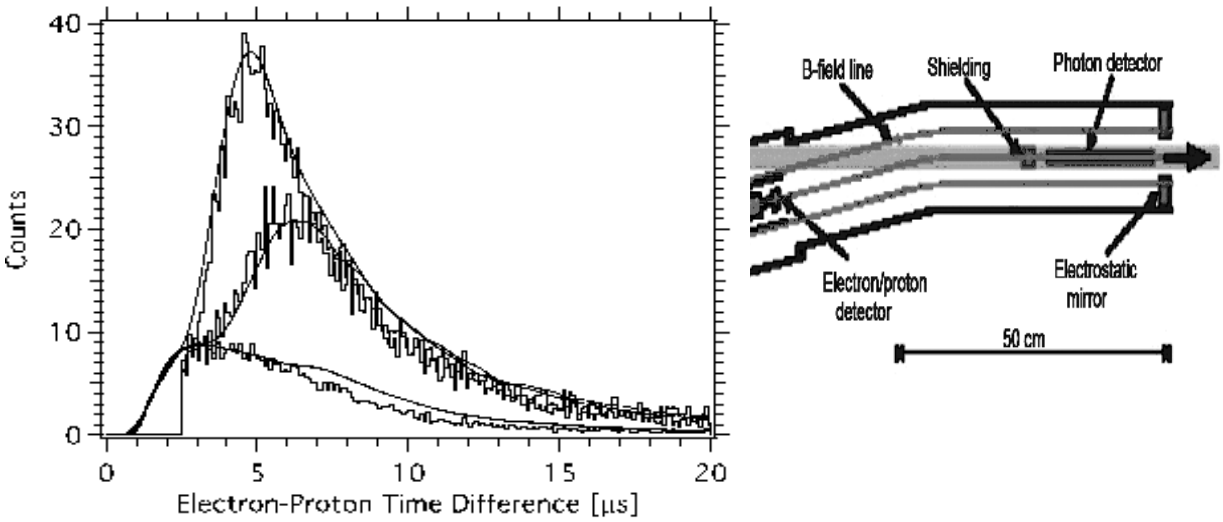

Fig. 6. On the right: the facility diagram. On the left: spectrum of double coincidences published in [12]. The lower curve corresponds to 0 volts, the middle curve corresponds to 300 volts and the highest curve corresponds to 500 volts in an electrostatic mirror. The location of the peak and its width differ from our and the emiT's results by one and two orders of magnitude. The location and the width of the peak also deviate by one and two orders of magnitude from the elementary estimates of the proton decay delay times.

Now we will compare our results and the results obtained by the emiT group with the third result, that is the spectrum of double coincidences obtained by another NIST group [12]. Unfortunately, the authors did not publish the spectrum of double coincidences in their original article [7], but published it much later [12]. Fig. 6 displays the spectrum on the left and the diagram of NIST experimental facility on the right. Fig. 6 clearly shows one single and a very wide peak with a long tail, which has nothing in common with either our peak or the emiT group peak.

The significant deviation obtained is explained by the fact that the peak in the NIST experiment consists not of protons but rather of ions. The density of gas molecules inside the experimental chamber is proportional to pressure and according to the Avogadro's Law is at the order of 10^{7}mol/cm^{3} even at the pressure of 10^{-8}–10^{-9} mbar. This is a very significant number, quite sufficient for creation of the large ionic background in the presence of ionizing radiation created in the chamber by beta-electrons of neutron decay. The energy of beta-electrons significantly exceeds the energy of ionization. Besides, as mentioned above, the probability of ionization is inverse proportional not to volume taken up by one molecule but to the average distance between molecules. It is precisely due to this reason that the ionic background falls much more gradually, proportionally to the cubic root of the pressure and not proportionally to the pressure. We observed a similar behavior of the ion background many times during our experiment; roughly speaking, if the pressure in the chamber dropped by an order of magnitude, the background decreased by only a factor of two or more. As mentioned above, comparing our results with those of the emiT group gives a drop in the ionic background of only 4–5 times, not two orders of magnitude. In the emiT group experiment the conditions were the same as in the second NIST group experiment, therefore the ionic background should be the same too. The light ions, together with the beta decay protons, should have a delay time comparable to 1 μs. The pulses from these particles are simply not visible in the spectrum due to the second NIST group's use of combined electron-proton detector in order to register both electrons and protons with ions. Fig. 6 shows a huge pulse from an electron, which simply "blinds" the detector for the time the small pulse from the proton and light ions arrives. The maximum of the ion peak in this group experiment, according to the delay times estimations (delay time is proportional to square root of ion mass), falls exactly to the 4–6 μs on the air ions consisting of nitrogen and oxygen.

Fig. 7 presents the pulse forms from the electron, ion, and gamma-quantum published by the second experimental group from NIST [7]. Firstly we should note the exceptionally long and flat front from the gamma pulse of 15 μs, which arises because of the extremely slow detectors on avalanche diodes. The authors used them because they used strong magnetic fields of several tesla, in which fast PECs do not work. As was pointed out above, a strong pulse from an electron makes weak pulses from ions and protons invisible during the first microseconds after its arrival. Namely this fact explains the dead zone around zero of the diagram in Fig. 6 which is where the pulses from the decay protons should come.

Let us now proceed to analysing of our triple coincidences spectra presented in Fig. 7. As it was mentioned above, both double coincidences spectra obtained by our (Fig. 4) and the emiT (Fig. 5) groups present two main peaks located on the horizontal ionic background. As for the spectrum of triple coincidences, we should observe not two but three peaks: one radiative peak and two peaks similar to the ones in the double coincidence diagram. Let us review this similarity in more detail: the peaks on the spectrum of double coincidences are as if transferred to the spectrum of triple coincidences.

We have two channels carrying background noise with some average signal frequency f_1 and f_2. Then the probabilities for the signal hitting the time window of value T are equal for both channels $p_1=f_1T$ and $p_2=f_2T$, respectively. If we now apply the electronic coincidence scheme, then the probability of random coincidence p_c of signals on the first and second channel in the coincidence scheme with the same value of time window T is equal to product of two independent events probabilities $p_c= p_1p_2= f_1Tf_2T$ and frequency of coincidence respectively is equal to $f_c=f_1f_2T$. Suppose now on the first channel there is not a homogeneous horizontal background of pulses with mean frequency f_1, but some input spectrum with its peaks S_{in} – then after the coincidence scheme an output spectrum proportional to the input $S_{out}= S_{in}f_2T$ with a ratio f_2T appears, note that the higher the homogeneous background on the second channel f_2, the more frequent the coincidence and the higher this ratio. Thus, all the peaks in the input spectrum also appear in the output spectrum from the coincidence scheme.

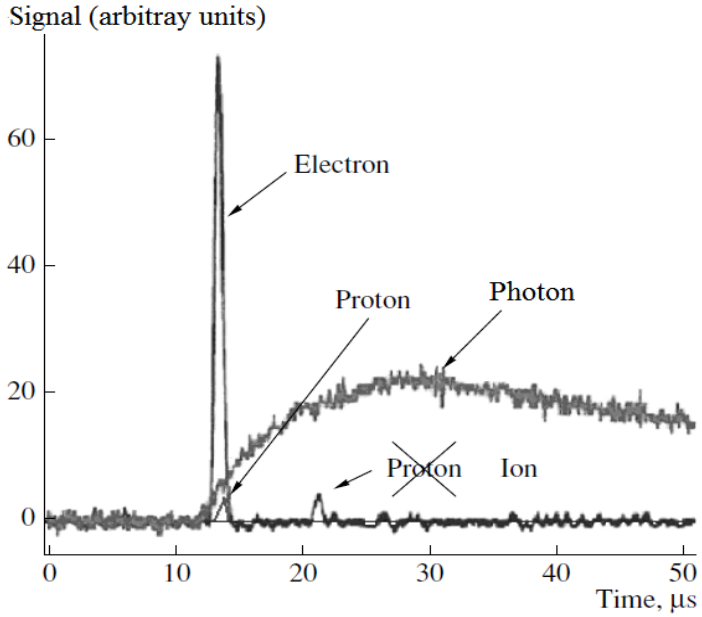

Fig. 7. The signal from the proton has to be delayed by less than one microsecond, which is why it is located at the base of the strong electron signal and so cannot be registered by the combined electron-proton detector. The pulses that are delayed by longer than 1 microsecond are pulses not from protons, as it was indicated in ref. [7], but rather from ions, formed in the viewed decay zone. A pulse from a photon has a front of about 15 μs.

However, simply multiplying the input spectrum by a number changes the height of the peak only, but both its width and its position remain unchanged. The real electronic coincidence circuit with the detector unit also makes hardware changes to the shape of the spectrum itself. Let us review these changes in more detail on our triple coincidence spectrum, shown in Fig. 8. The figure shows three peaks: the leftmost peak of triple coincidences located in channel 103, which consists of the supposed number of neutron radiative decay events we measure; two peaks from the input spectrum of double coincidences. These are the response peaks to the registration peak of electrons and delayed protons, respectively, but both response peaks on the spectrum of triple coincidences are significantly wider and located closer to each other than in the original spectrum of double coincidences (Fig. 4). These two wide peaks in channels 106 and 120 converge so that there is a rather high jumper between them. In addition, there is a small parasitic electron peak, the

nature of which is related to the electronic circuitry of the registration of gamma-quantum pulses.

Such distortions of the output spectrum are controlled by a standard procedure, introducing a response function for gamma channel $R_\gamma(t,t')$ [6] , which is also necessary for calculating the number of triple coincidences N_T in radiative peak:

$$S_{out}(t) = \int S_{in}(t')R_\gamma(t,t')dt'.$$

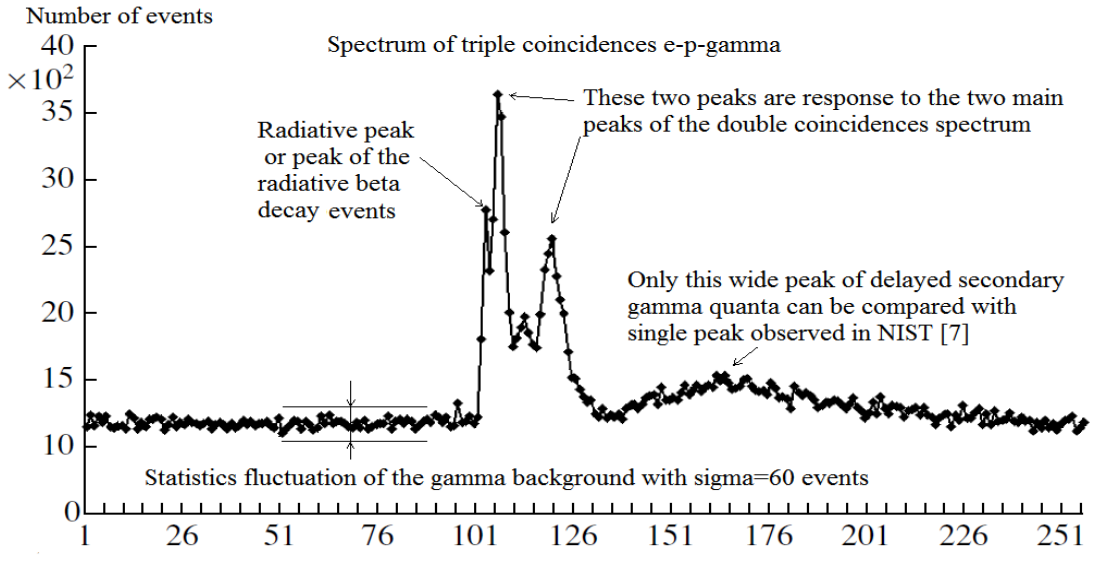

Fig. 8. Timing spectrum for triple e-p-γ coincidences. Each channel corresponds to 25 ns. In this spectrum, three main peaks in channels 103, 106 and 120 can be distinguished. The leftmost peak in channel 103 among these three main peaks is connected with the peak of radiative decay events.

This functional multiplication instead of simple multiplication of the input spectrum by a number takes into account all the distortions of the real spectrum. Namely, the response function method is able to consider both the change of the peak width and the convergence of two response peaks located around channels 106 and 120. In a particular case, if we use the local response function with zero width as a δ-function with some coefficient, it becomes a simple multiplication of the input spectrum by the number mentioned above. If we use the non-local response function then its width will lead to an increase in the widths of the response peaks, roughly speaking, by the width of the response function, and its tails will lead to a convergence of the peaks in the output spectrum compared to the original spectrum. This is exactly the picture we observe when comparing our double and triple coincidence spectra in Figs. 4 and 8. Thus, using the method of nonlocal response function we can distinguish the peak of radiative gammas on inhomogeneous double-humped background.

As for the wide peak in channel 165, it has a physical nature, has nothing in common with the peak of radiative decay and is well distinguished from it delaying at a considerable distance of 1 μs from it. This peak is created by the radioactive gamma quanta and emitted during ionization of rare atmosphere within our experimental chamber. The molecular of this medium is ionized by registered beta-electrons. This event is well studied and does not have anything in common with the new event of radiative neutron decay but happens due to the ionization of highly rarefied air by charged particles. It is this phenomenon that was observed

by the second NIST group, who published a single peak shown in Fig. 9 (see [7]). Let us note that the spectrum published by these authors is not a spectrum of triple coincidences; otherwise, as mentioned above, it would have had additional response peaks from the spectrum of double coincidences of the electron with the recoil proton, or, as in their case, with the ions. In fact, this experiment used everything needed to investigate the phenomenon known as polar lights. Firstly, it is the residual rarefied air, whose density just corresponds to the density of air at heights of 150–200 km, where natural polar lights occur; secondly, it is the presence of ionizing radiation in the form of beta electrons, flying from an intense beam of cold neutrons; and thirdly, it is the presence of magnetic fields. Thus, the authors of this experiment measured the relative intensity as the ratio of gamma-quanta produced by the ionization of air molecules to the total number of ions flying out of the same viewed decay zone under the influence of the electrostatic field. This ratio is also proportional to the fine structure constant $\alpha = 1/137$ and thus has the same order of magnitude as the BR in the case of neutron radiative decay.

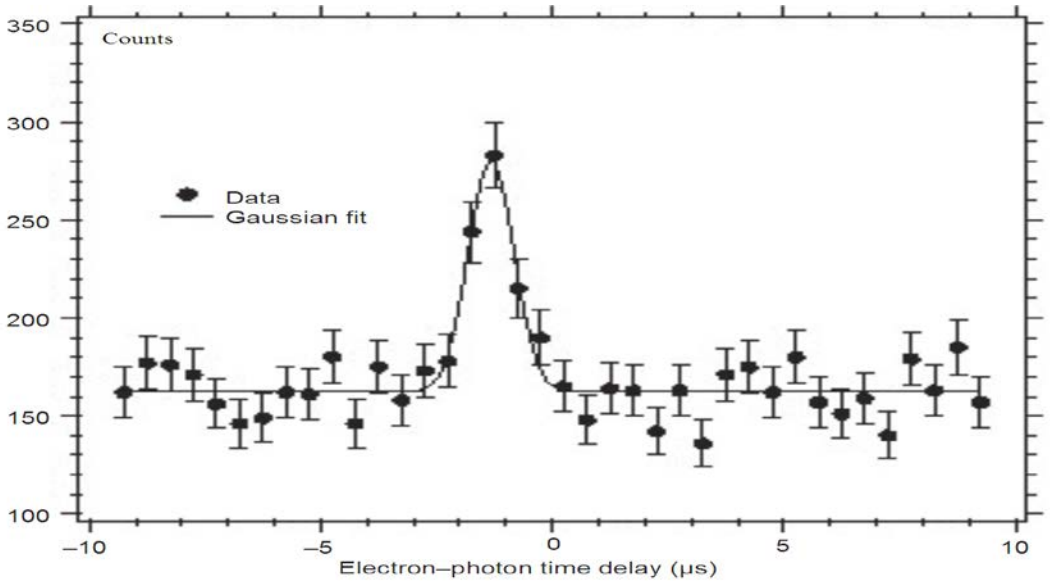

Fig. 9. The single peak of "electron-photon" coincidences, shifted to the left of 0 – the time of electron registration – by 1 μs, published in [7, 8]. On the spectrum of triple coincidences (see Fig. 8) in our experiment a similar wide peak is located after the electron registration and there are no wide peaks before the beta-electron registration.

After analyzing triple coincidences spectra with the help of the non-local response function $R_\gamma(t,t')$, we finalize the number of radiative neutron decays N_T=360 with a statistics fluctuation of 60 events. B.R. can be expressed as a ratio of N_T to N_D as $BR = N_T / N_D/k$, where coefficient k=0.3 is the geometrical factor that we can calculate by using geometry of the facility as well as anisotropic emission of radiative gamma-quanta during neutron decay [4]. With the number of observed double e-p coincidences $N_D = 3.75 \cdot 10^5$ and triple e-p-γ coincidences $N_T = 360$, one can deduce the value for the main characteristics of neutron decay, branching ratio $B.R.= (3.2 \pm 1.6) \cdot 10^{-3}$ (99.7 % C.L.) with the threshold gamma energy ω=35 keV. In this case we chose C.L.= 99.7%, which corresponds to an error of 3σ, and the resulting error was 50% of the mean B.R. If, however, we choose the standard confidence limit C.L.= 68% with an error of 1σ, the error is only 15% of the mean value. On the other

hand, this experimental mean of B.R.= 3.2 is 1.5 times higher than that calculated by the standard model of electroweak interaction. This means that approximately one-third of the gamma quanta we recorded are structural.

To conclude our review of the time coincidence spectra, it is appropriate to note again that it would be extremely naive to expect to see one single isolated peak of triple coincidences on the spectrum, Fig. 8, the value of which determines the number of registered neutron radiation decays. As can be seen in the block diagram of our data acquisition and processing system, Fig. 3, the signals from the gamma-ray detector are fed to the triple coincidence circuit directly. It is obvious that such an ideal picture of one single isolated peak is possible only in the ideal case where the gamma background is absent. In the real experiment, however, the gamma background is not only significant but also has its own peaks. Given its presence on the final spectrum of triple coincidences, all peaks of double coincidence spectra should appear, in our case the spectrum of double electron-proton coincidences and the spectrum of double electron-gamma coincidences – we see these peak responses on the real spectrum of triple coincidences of electron, proton and gamma-quantum.

Conclusions

The main result of our experiment is the identification of neutron radiative decay events. The location and the width of the radiative peak correspond both to the estimates and the detailed Monte Carlo simulation of the experiment. We measured the relative intensity of rare neutron decay mode, B.R.= $(3.2\pm0.53)\cdot10^{-3}$ (with C.L.=68% and gamma quanta energy over 35 keV). It means that the average experimental B.R. value exceeds the theoretical one calculated within the standard electroweak model by 1.5 times. At the same time, the deviation of the theoretical and experimental relative intensities exceeds the standard error of 1σ. This fact means that the experiment detected additional structural gamma quanta, which are now emitted by the quark structure of the neutron during the transition of d quark to u quark. As follows from the comparison of experimental and theoretical values of the relative intensity of radiative gammas emitted during neutron decay, every third registered radiative gamma-quantum is a structural one.

In order to confirm and more accurately determine the intensity of structural gamma quanta emission, it is necessary to conduct a new experiment with a larger volume of collected statistics and with a lower threshold of energies of registered gamma quanta. We prepared such experiment several years ago, however, due to the lack of a PIK research neutron reactor, we cannot conduct it on an intense beam of cold neutrons.

The comparison of our results with emiT group's results on the spectra for regular neutron decay shows a complete coincidence. Both we and the emiT group obtained identical double-coincidence spectra with two peaks on the horizontal ionic background. We are very pleased to state this fact. Unfortunately, we cannot say same for another NIST group which claims to measure the relative intensity of neutron radiative decay.

Not only do they not register triple coincidences, without which it is impossible to talk about the measurement of B.R., but they also cannot register neutron radiative decay events at all. Instead, the authors of the experiment study the emission of gamma quanta by residual air molecules in the chamber when they are ionized by beta electrons from neutron decay. This process is well studied and has nothing to do with neutron radiative decay. In nature, this effect of ionization of rarefied air by electrons is observed in the form of polar lights. At the same time, as can be seen from our triple coincidence spectrum in Fig. 8, this peak of delayed gamma quanta is located after electron registration with a considerable delay of the order of

1μs and is well distinguished from the peak of neutron radiative decay. This result is in a sharp contradiction with the result of NIST group which published their only peak of double electron-gamma coincidence also for 1 microsecond, however not after, but before electron registration (see Fig. 9). That is in a sharp contradiction with results of elementary evaluations, this peak simply could not appear, if it is located at such a large distance before the electron registration. We consider the location of the peak of the double electron-gamma coincidences as suggested by the authors of the contribution to Nature [7] as a sheer misrepresentation, and we understand how it happened [13]. We strongly recommend that the NIST researches withdraw their contribution to Nature and submit a new one where the only peak of the double electron-gamma coincidences is located where they actually observe it in the same 1 microsecond - not before but after the electron registration.

We express our sincere gratitude to NRC «Kurchatov Institute» Honorary President Academician E.P. Velikhov for his support, without which we would not have been able to conduct our experiments on neutron radiative decay, neither in France at ILL, nor in Germany at TUM. We would like to thank Academician S.S. Gerstein and Professor P. Depomier of Montreal University for their interest and discussions of our work.

References

1. Gaponov Yu.V., Khafizov R.U., Phys. Lett. B 379 (1996) 7–12.
2. Yu.V. Gaponov, R.U. Khafizov, *Radiative neutron beta-decay and experimental neutron anomaly problem.* Weak and electromagnetic interactions in nuclei (WEIN '95): proceedings. Edited by H. Ejiri, T. Kishimoto, T. Sato. River Edge, NJ, World Scientific, 1995, 745p.
3. R.U. Khafizov, N. Severijns, *About the possibility of conducting an experiment on radiative neutron beta decay*, in Proceedings of VIII International Seminar on Interaction of Neutrons with Nuclei (ISINN-8), Dubna, May 17–20, 2000, E3-2000-192, 185–195.
4. Khafizov R.U. Physics of Particles and Nuclei, Letters 108 (2001) 45–53.
5. M. Beck, J. Byrne, R.U. Khafizov, et al., JETP Letters 76, 2002, p. 332.
6. R.U. Khafizov, N. Severijns, O. Zimmer et al. JETP Letters 83 (2006) p. 5.
7. J.S. Nico, et al. Nature, v. 444 (2006) p. 1059–1062.
8. M.J. Bales, R. Alarcon, C.D. Bass, et al., Phys. Rev. Lett. 116 (2016), 242501.
9. B.G. Yerozolimsky, Yu.A. Mostovoi, V.P. Fedunin, et al., Yad. Fiz. 28, 98(1978); [Sov. J. Nucl. Phys. 28, 48 (1978)].
10. I.A. Kuznetsov, A.P. Serebrov, I.V. Stepanenko, et al., Phys. Rev. Lett., 75. (1995) 794.
11. L.J. Lising, S.R. Hwang, J.M. Adams, et al., Phys. Rev. C., v.6, 2000, p. 055501.
12. R.L. Cooper, T.E. Chupp, M.S. Dewey, et al., Phys. Rev. C 81, 2010, p. 035503.
13. N. Severijns. Nature, v. 444 (2006), p. 1014–1015.